

doi: 10.15407/ujpe62.02.0152

H.H. KHUDHER,¹ A.K. HASAN,¹ F.I. SHARRAD²

¹ Department of Physics, Faculty of Education for Girls, University of Kufa
(31001 Najaf, Iraq; e-mail: fadhil.altaie@gmail.com)

² Department of Physics, College of Science, University of Kerbala
(56001 Karbala, Iraq; e-mail: fadhil.altaie@gmail.com)

CALCULATION OF ENERGY LEVELS, TRANSITION PROBABILITIES, AND POTENTIAL ENERGY SURFACES FOR $^{120-126}\text{Xe}$ EVEN-EVEN ISOTOPES

PACS 21.60.Ev, 27.70.+q,
23.20.-g, 23.20.Lv

The interacting boson model (IBM-1) is used to calculate the energy levels, transition probabilities $B(E2)$, and potential energy surfaces of some even $^{120-126}\text{Xe}$ isotopes. The theoretical values are in good agreement with the experimental data. The potential energy surface is one of the nucleus properties, and it gives a final shape of nuclei. The contour plot of the potential energy surfaces shows that the $^{120-126}\text{Xe}$ nuclei are deformed and have γ -unstable-like characters.

Keywords: IBM-1, energy levels, $B(E2)$ values, potential energy surface, Xe isotopes.

1. Introduction

The interacting boson model represents an important step to understand the nuclear structure. It introduces a simple Hamiltonian capable of describing collective nuclear properties through an extensive range of nuclei, and it is based on somewhat general algebraic group theoretical methods [1, 2]. The interacting boson model-1 (IBM-1) is a valuable interactive model developed by Iachello and Arima [3, 4]. It has been efficient in describing the collective nuclear structure of the medium-mass nuclei, low-lying states, and electromagnetic transition rates. The interacting boson model defines the six-dimensional space and is described by in terms of the unitary group $U(6)$.

There are three dynamical symmetry limits of $U(6)$ known as a spherical vibrator, symmetric rotor, and γ -unstable rotor which are labeled by $U(5)$, $SU(3)$, and $O(6)$, respectively [5, 6]. Xenon isotopes belong to a very exciting, but complex region of the Periodic table known as the transition region. The xenon isotopes can exhibit the excitation spectra close to the $O(6)$ symmetry. Xenon isotopes are in a typical transition region of nuclei, in which the nuclear structure varies from that of a spherical nucleus to a deformed nucleus [7]. For the xenon series of isotopes, the original version of IBM-1 had been used in calculating

the energy levels of the positive parity low-lying nuclei [8]. For the even $^{120-126}\text{Xe}$ isotopes with neutron number ($66 \leq N \leq 72$), the energy ratio ($E4^+/E2^+$) is nearly 2.5 and indicates γ -soft shapes. In the recent years, many works had been done on the structure of xenon isotopes; S.A. Eid and S.M. Diab [9] calculated the potential energy surfaces, $(V\beta, \gamma)$ for a series of xenon isotopes $^{122-134}\text{Xe}$, energy levels, and reduced transition probabilities $B(E2)$, by using IBM-1. These results were compared with the experimental data and found sensible agreement. K. Pomorski and B. Nerlo-Pomorska [10] studied the quick rotation for the even-even Zn, Mo, Sn, Te, Xe, Ba, Ce, and Nd isotopes and presented the typical properties for high-spin states as well. B.S. Rawat and P.K. Chattopadhyay [11] analyzed the spectra of the xenon isotopes by the $O(6)$ symmetry breaking and used the excitation energies of the states 0_2^+ and 0_3^+ under a noticeable breaking of the symmetry. H. Kusakari and M. Sugawara [12] calculated the energy levels, backbendings in the yrast bands, and reduced transition probabilities for the positive-parity states of $^{122-130}\text{Xe}$ within the framework of the interacting boson model. B. Saha *et al.* [13] measured the $B(E2)$ and $B(M1)$ values for the isotope of ^{124}Xe . H. Kusakari *et al.* [14] studied the high-spin states in the even $^{122-130}\text{Xe}$ by in-beam γ -ray spectroscopy. The 10_2^+ level in ^{126}Xe was assigned

near the 10_1^+ level, and the 14_2^+ level was too. In the yrast bands, the backbending phenomena were detected systematically in the even $^{122-130}\text{Xe}$ isotopes. L. Coquard *et al.* [15] investigated low-lying collective states in ^{126}Xe via the $^{12}\text{C}(^{126}\text{Xe}, ^{126}\text{Xe}^*)$ projectile Coulomb excitation reaction at 399 MeV. M. Serris *et al.* [16] used the EUROGAM array to investigate the high-spin states in ^{122}Xe by $\gamma - \gamma$ coincidence measurements. The reaction ^{96}Zr (^{30}Si , $4n$) ^{122}Xe was used to populate states of ^{122}Xe at a beam energy of 135 MeV. The new structures of competing $B(M1)$ to $B(E2)$ transitions were observed. In the $O(6)$ -like nuclei, the triaxial deformation of the even-even Xe, Ba, Ce isotopes had been studied.

The aim of the present work is to study the energy levels, transition probabilities $B(E2)$, and the potential energy surfaces of some even $^{120-126}\text{Xe}$ isotopes within the framework of IBM-1 and to compare the results with the experimental data. Furthermore, we will describe the nuclear structure for Xe isotopes, by using the potential energy surface $E(N, \beta, \gamma)$.

2. Interacting Boson Model (IBM-1)

The Interacting Boson Model has become one of the most intensively used nuclear models, due to its ability to describe the changing low-lying collective properties of nuclei across the entire major shell with a simple Hamiltonian. In IBM-1, the low-lying collective properties of even-even nuclei were described in terms of a system of interacting s -bosons ($L = 0$) and d -bosons ($L = 2$) [18]. The underlying structure of the six-dimensional unitary group $U(6)$ of the model leads to a simple Hamiltonian capable of describing the three dynamical symmetries $U(5)$, $SU(3)$, and $O(6)$ [4, 18]. The most general IBM Hamiltonian can be expressed as [19, 20]:

$$\begin{aligned} H = & \varepsilon_s(s^\dagger \cdot \tilde{s}) + \varepsilon_d(d^\dagger \cdot \tilde{d}) + \sum_{L=0,2,4} \frac{1}{2}(2L+1)^{1/2} C_L \times \\ & \times \left[[d^\dagger \times d^\dagger]^{(L)} \times [\tilde{d} \times \tilde{d}]^{(L)} \right]^{(0)} + \frac{1}{\sqrt{2}} v_2 \left[[d^\dagger \times d^\dagger]^{(2)} \times \right. \\ & \times [\tilde{d} \times \tilde{s}]^{(2)} + [d^\dagger \times s^\dagger]^{(2)} \times [\tilde{d} \times \tilde{d}]^{(2)} \left. \right]^{(0)} + \\ & + \frac{1}{2} v_0 \left[[d^\dagger \times d^\dagger]^{(0)} \times [\tilde{s} \times \tilde{s}]^{(0)} + [s^\dagger \times s^\dagger]^{(0)} \times \right. \\ & \times [\tilde{d} \times \tilde{d}]^{(0)} \left. \right]^{(0)} + \frac{1}{2} u_0 \left[[s^\dagger \times s^\dagger]^{(0)} \times [\tilde{s} \times \tilde{s}]^{(0)} \right]^{(0)} + \\ & + u_2 \left[[d^\dagger \times s^\dagger]^{(2)} \times [\tilde{d} \times \tilde{s}]^{(2)} \right]^{(0)}, \end{aligned} \quad (1)$$

where (s^\dagger, d^\dagger) and (\tilde{s}, \tilde{d}) are the creation and annihilation operators for s - and d -bosons, respectively [18]. This Hamiltonian contains two one-body terms specified by the parameters $(\varepsilon_s$ and ε_d) and seven two-body terms specified by the parameters $[C_L (L = 0, 2, 4), v_L (L = 0, 2), u_L (L = 0, 2)]$, where ε_s and ε_d are the single-boson energies, and c_L , v_L and u_L describe the two-boson interactions. However, it turns out that, for a fixed boson number N , only one of the one-body terms and five of the two-body terms are independent, as it can be seen by noting $N = n_s + n_d$. There are several corresponding ways to write the Hamiltonian, one of these forms is the multipole expansion [18, 19, 20]

$$\hat{H} = \varepsilon \hat{n}_d + a_0 \hat{p} \cdot \hat{p} + a_1 \hat{L} \cdot \hat{L} + a_2 \hat{Q} \cdot \hat{Q} + a_3 \hat{T}_3 \cdot \hat{T}_3 + a_4 \hat{T}_4 \cdot \hat{T}_4. \quad (2)$$

The operators are defined by the following equations:

$$\hat{n}_d = (d^\dagger \tilde{d}), \quad (3)$$

$$\hat{p} = 1/2[\tilde{d}, \tilde{d} - \tilde{s}, \tilde{s}], \quad (4)$$

$$\hat{L} = \sqrt{10}[d^\dagger \times \tilde{d}]^1, \quad (5)$$

$$\hat{Q} = [d^\dagger \times \tilde{s} + s^\dagger \times \tilde{d}]^{(2)} + \chi [d^\dagger \times \tilde{d}]^{(2)}, \quad (6)$$

$$\hat{T}_r = [d^\dagger \times \tilde{d}]^{(r)}, \quad (7)$$

$$\varepsilon = \varepsilon_d + \varepsilon_s, \quad (8)$$

where \hat{n}_d , \hat{p} , \hat{L} , \hat{Q} , and \hat{T}_r are the total number of d -bosons, pairing, angular momentum operator, quadrupole, octupole ($r = 3$), and hexadecapole ($r = 4$) operators, respectively, ε is the boson energy, and χ (CHI) is the quadrupole structure parameter, which takes the values 0 and $\pm \frac{\sqrt{7}}{2}$ [18, 19, 20]. The parameters a_0 , a_1 , a_2 , a_3 , and a_4 designate the pairing strength, angular momentum, quadrupole, octupole, and hexadecapole interactions between the bosons. The $O(6)$ symmetry of IBM-1 is based on the chain $U(6) \supset O(6) \supset O(5) \supset O(3)$ of the nested subalgebra with quantum numbers N , σ , and L , respectively [18]. The energies of collective states in the $O(6)$ limit are given by [18];

$$\begin{aligned} E(\sigma, \tau, L) + A(N - \sigma)(N + \sigma + 4) + \\ + B\tau(\tau + 3) + CL(L + 1), \end{aligned} \quad (9)$$

where ($A = a_0/4$, $B = a_3/2$, $C = a_1 - a_3/10$), N is the number of bosons $\sigma = N, N - 2, N - 4, \dots, 0$ and

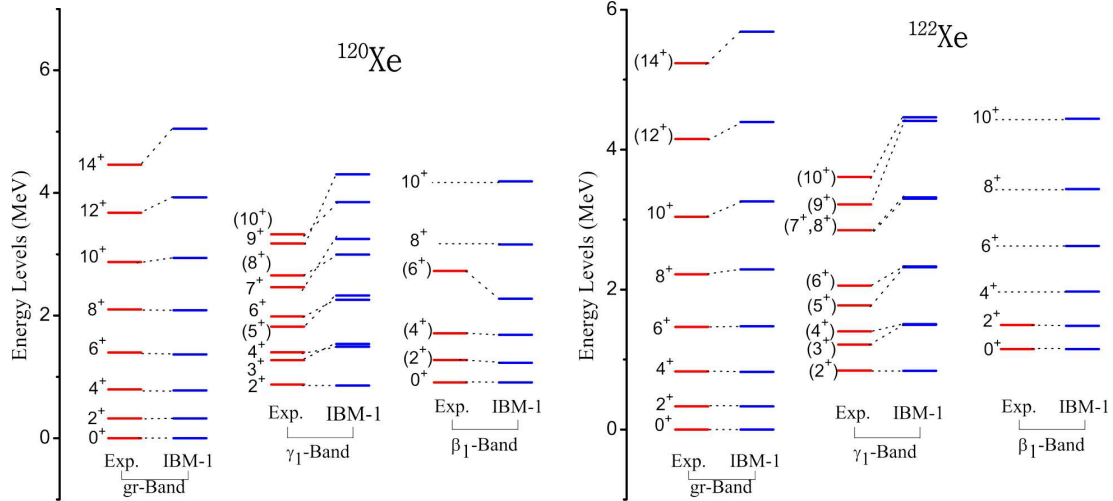


Fig. 1. (Color Online) Comparison the IBM-1 calculations with the available experimental data [22–24] for $^{120-122}\text{Xe}$ nuclei

Table 1. Adopted values of the parameters used in the IBM-1 calculations. All parameters are given in MeV, except N and CHI (CHI is a constant dependent on the dynamical symmetry)

Isotope	N	ε	a_0	a_1	a_2	a_3	a_4	CHI
^{120}Xe	10	0.0000	0.082609	0.012133	0.0000	0.178435	0.0000	0.0000
^{122}Xe	9	0.0000	0.114918	0.015834	0.0000	0.168768	0.0000	0.0000
^{124}Xe	8	0.0000	0.14099	0.019322	0.0000	0.170068	0.0000	0.0000
^{126}Xe	7	0.0000	0.164235	0.022538	0.0000	0.181002	0.0000	0.0000

$\tau = 0, 1, \dots, \sigma$. L takes on the $L = 2\lambda, 2\lambda - 2, \dots, \lambda + 1, \lambda$, where λ is a positive integer; $\lambda = \tau - 3v_\Delta$ for $v_\Delta = 0, 1, 2, \dots$ [20].

3. Results and Discussion

The calculated results can be discussed separately for the energy levels, reduced probability of $E2$ transitions, and potential energy surfaces.

3.1. Energy Levels

The energy levels of some even $^{120-126}\text{Xe}$ isotopes have been calculated, by using the experimental energy ratios $E2:E4:E6:E8 = 1:2.5:4.5:7$ [21] within the framework of IBM-1. It has been found that the $^{120-126}\text{Xe}$ isotopes are deformed nuclei, and they have a dynamical symmetry $O(6)$. For the analysis of excitation energies of xenon isotopes, it is tried to keep a minimum number of free parameters in the Hamiltonian. The adopted Hamiltonian is expressing

as [20]

$$\hat{H} = a_0 \hat{P} \cdot \hat{P} + a_1 \hat{L} \cdot \hat{L} + a_3 \hat{T}_3 \cdot \hat{T}_3. \quad (10)$$

In IBM-1, the even $^{120-126}\text{Xe}$ isotopes ($Z = 54$) have a number of proton boson particles equal to 2, and a number of neutron boson holes varies from 5 to 8, respectively. The Table 1 shows that the parameters used in the present work. The calculated ground g -band, β -band, and γ -band and the experimental data on low-lying states are plotted in Figs. 1 and 2 for even-even $^{120-126}\text{Xe}$ isotopes. These figures show that the IBM calculations of the energies, spin, and parity are in good agreement with the experimental values [22–26]. However, it is deviated in the high-spin energies of the experimental data. Levels with ‘()’ correspond to the cases, for which the spin and/or parity of the corresponding states are not well established experimentally.

Furthermore, from Fig. 1, the levels 5_1^+ , 8_2^+ , 10_2^+ , 2_3^+ , 4_3^+ , and 6_3^+ with energies of 2.326, 2.996, 3.850,

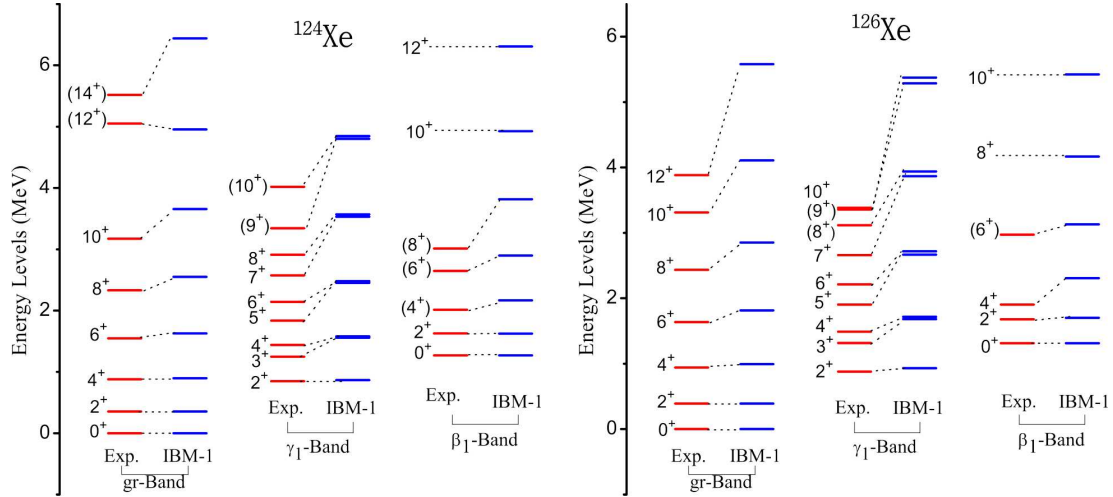


Fig. 2. (Color Online) Comparison the IBM-1 calculations with the available experimental data [22, 25, 26] for $^{124-126}\text{Xe}$ nuclei

Table 2. β_2 -bands for Xe isotopes (in MeV). The experimental data are taken from [22–26]

J^π	^{120}Xe		^{122}Xe		^{124}Xe		^{126}Xe	
	IBM-1	exp.	IBM-1	exp.	IBM-1	exp.	IBM-1	exp.
0+	1.6051	1.62325	1.5210	2.26444 *	1.5300	1.68991	1.6290	1.76054
2+	1.9746	1.92411 *	2.3597	2.3431	2.3938	2.51947	2.5607	2.45533
4+	2.4000	2.44842 *	2.6500	—	2.8450	—	3.0316	2.9739 *
6+	3.1667	—	3.4719	—	3.7456	—	4.0345	—
8+	4.0663	—	4.4544	—	4.8016	—	5.2540	—
10+	5.0987	—	5.5975	—	6.2030	—	—	—

1.231, 1.688, and 2.275 MeV, respectively, for ^{120}Xe isotope, and 12_1^+ , 14_1^+ , 2_2^+ , 3_1^+ , 4_2^+ , 5_1^+ , 6_2^+ , 7_1^+ , 8_2^+ , 9_1^+ , and 10_2^+ with energies of 4.3992, 5.6945, 0.8387, 1.5084, 1.500, 2.3345, 2.3219, 3.3212, 3.3044, 4.4685, and 4.4145 MeV, respectively, for ^{122}Xe isotope correspond to the cases, for which the spin and/or parity of the corresponding states are not well established experimentally [22–24]. From Fig. 2, the levels 12_1^+ , 14_1^+ , 9_1^+ , 10_2^+ , 4_2^+ , 6_3^+ , and 8_3^+ with energies of 4.9488, 6.4330, 4.7970, 4.8430, 2.1650, 2.8956, and 3.8146 MeV for ^{124}Xe isotope, and 8_2^+ , 9_1^+ , and 6_3^+ with energies of 3.9404, 5.2875, and 3.1295 MeV for ^{126}Xe isotope correspond to the cases, for which the spin and/or parity of the corresponding states are not well established experimentally [22, 25, 26]. The β_2 -bands calculated in this work are shown in Table 2. This table presents the comparison between of

the IBM-1 calculations and the experimental energy levels of $^{120-126}\text{Xe}$ isotopes. From this comparison, a good agreement between the experimental data and the IBM-1 calculation is seen. Levels with '*' correspond to cases, for which the spin and/or parity of the corresponding states are not well established experimentally.

3.2. The $B(E2)$ Values

New information can be founded, by studying the reduced transition probabilities $B(E2)$. The reduced matrix elements of the $E2$ operator have the form [18, 27, 28]

$$\begin{aligned} \hat{T}(E2) &= \alpha_2[d^\dagger \tilde{s} + s^\dagger \tilde{d}]^{(2)} + \beta_2[d^\dagger \tilde{d}]^{(2)} = \\ &= \alpha_2([d^\dagger \tilde{s} + s^\dagger \tilde{d}]^{(2)} + \chi[d^\dagger \tilde{d}]^{(2)}) = e_B \hat{Q}, \end{aligned} \quad (11)$$

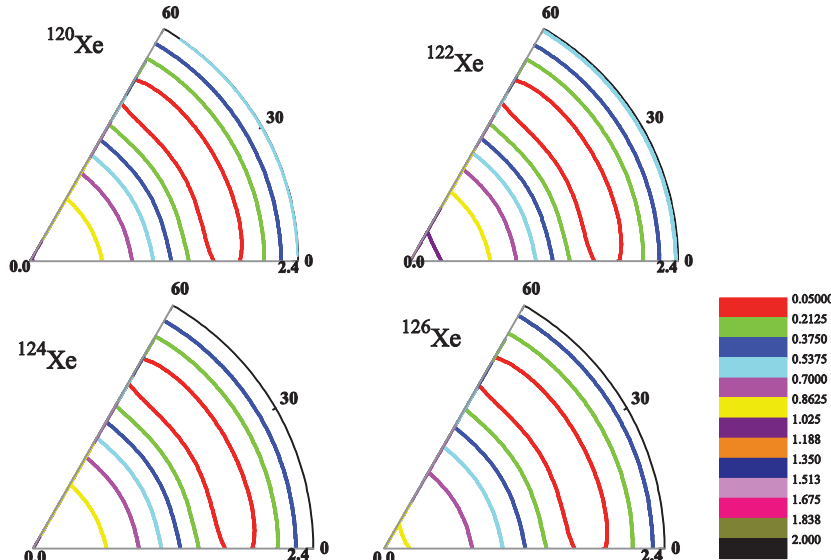


Fig. 3. Color Online) Potential energy surface in the $\gamma - \beta$ plane for $^{120-126}\text{Xe}$ nuclei

where α_2 and β_2 are two parameters, $\beta_2 = \chi\alpha_2$, $\alpha_2 = e_B$, where e_B is the effective charge, and

$$\hat{Q} = ([d^\dagger \tilde{s} + s^\dagger \tilde{d}] + \chi[d^\dagger \tilde{d}]^{(2)}), \quad (12)$$

where \hat{Q} is the quadrupole operator. The electric transition probabilities $B(E2)$ are defined in terms of reduced matrix elements as [18, 30]

$$B((e2), J_i \rightarrow J_f) = \frac{1}{2J_i} \left| \langle J_f \parallel \hat{T}(E2) \parallel J_i \rangle \right|^2. \quad (13)$$

The values e_B are estimated to reproduce the experimental $B(E2; 2_1^+ \rightarrow 0_1^+)$ and are given in Table 3. In addition, the comparisons of the calculated $B(E2)$ values with the experimental data [22–26] are given in Table 4 for all nuclei under study.

Table 4 shows that, in general, most of the calculated results in IBM-1 are reasonably consistent with the available experimental data, except for few cases that deviate from the experimental data.

Table 3. Effective charge used to reproduce $B(E2)$ values for $^{120-126}\text{Xe}$ Nuclei

A	N	e_B (eb)
^{120}Xe	10	0.1112
^{122}Xe	9	0.1094
^{124}Xe	8	0.10
^{126}Xe	7	0.10

3.3. Potential energy surface $E(N, \beta, \gamma)$

The potential energy surface gives a final shape to the nucleus that corresponds to the Hamiltonian [31] in the equation [20]

$$E(M, \beta, \gamma) = \langle N, \beta, \gamma | H | N, \beta, \gamma \rangle / \langle N, \beta, \gamma | N, \beta, \gamma \rangle. \quad (14)$$

The expectation value of the IBM-1 Hamiltonian with the coherent state ($|N, \beta, \gamma\rangle$) is used to construct the IBM energy surface [19, 20]. The state is a product of boson creation operators,

$$(b_c^\dagger), \quad \text{with} \quad |N, \beta, \gamma\rangle = 1/\sqrt{N!} (b_c^\dagger)^N |0\rangle, \quad (15)$$

$$b_c^\dagger = (1 + \beta^2)^{-1/2} \{ s^\dagger + \beta[\cos \gamma(d_0^\dagger) + \sqrt{1/2} \sin \gamma(d_2^\dagger + d_{-2}^\dagger)] \}. \quad (16)$$

The energy surface, as a function of β and γ , has been given by [18]

$$E(N, \beta, \gamma) = \frac{N\varepsilon_d \beta^2}{(1 + \beta^2)} + \frac{(N(N+1))}{(1 + \beta^2)^2} \times \times (\alpha_1 \beta^4 + \alpha_2 \beta^3 \cos 3\gamma + \alpha_3 \beta^2 + \alpha_4), \quad (17)$$

where the α_i are related to the coefficients C_L , ν_2 , ν_0 , u_2 , and u_0 of Eq (1), and β is a measure of the total deformation of a nucleus. For $\beta = 0$, the shape

Table 4. $B(E2)$ values for $^{120-126}\text{Xe}$ nuclei (in $e^2\text{b}^2$)

$J_i \rightarrow J_f$	^{120}Xe [22, 23]		^{122}Xe [22, 24]		$J_i \rightarrow J_f$	^{124}Xe		^{126}Xe	
	IBM-1	exp.	IBM-1	exp.		IBM-1	exp. [22, 25, 32]	IBM-1	exp. [22, 26, 32]
$2_1^+ \rightarrow 0_1^+$	0.3460	0.346(22)	0.2800	0.280(12)	$2_1^+ \rightarrow 0_1^+$	0.1920	0.192(12)	0.1540	0.154(5)
$2_2^+ \rightarrow 0_1^+$	0.0483	–	0.0392	–	$2_2^+ \rightarrow 0_1^+$	0.0270	0.0026(5)	0.0217	0.002(7)
$2_2^+ \rightarrow 2_1^+$	0.4766	–	0.3829	–	$4_1^+ \rightarrow 2_1^+$	0.2600	0.2484(7)	0.2057	0.267(3)
$4_1^+ \rightarrow 2_1^+$	0.4766	0.412(28)	0.3829	0.409(22)	$4_2^+ \rightarrow 2_1^+$	0.0206	0.00025	0.0160	0.0015(3)
$4_2^+ \rightarrow 2_1^+$	0.0385	–	0.0307	–	$4_2^+ \rightarrow 2_2^+$	0.1467	0.254(92)	0.1135	0.1355(16)
$6_1^+ \rightarrow 4_1^+$	0.5272	0.415(63)	0.4188	0.396(144)	$6_1^+ \rightarrow 4_1^+$	0.2800	0.323(29)	0.2167	0.315(41)
$6_2^+ \rightarrow 4_1^+$	0.0295	–	0.228	–	$6_2^+ \rightarrow 4_1^+$	0.0147	–	0.0108	–
$6_1^+ \rightarrow 4_2^+$	0.0245	–	0.0211	–	$4_2^+ \rightarrow 6_1^+$	0.0228	–	0.0204	–
$8_1^+ \rightarrow 6_1^+$	0.5347	0.341(59)	0.4177	0.288(179)	$8_1^+ \rightarrow 6_1^+$	0.2727	0.243(77)	0.2036	–
$8_1^+ \rightarrow 6_2^+$	0.0289	–	0.0225	–	$8_1^+ \rightarrow 6_2^+$	0.0195	–	0.0179	–
$10_1^+ \rightarrow 8_1^+$	0.5133	0.324(53)	0.3912	0.432(179)	$10_1^+ \rightarrow 8_1^+$	0.2462	0.0772(1)	0.1731	–
$10_2^+ \rightarrow 10_1^+$	0.0046	–	0.0032	–	$12_1^+ \rightarrow 10_1^+$	0.2040	0.202(44)	0.1280	–
$12_1^+ \rightarrow 10_1^+$	0.4695	0.292(46)	0.3446	–	$2_2^+ \rightarrow 2_1^+$	0.2600	0.118(22)	0.2057	0.162(1)
$12_2^+ \rightarrow 10_2^+$	0.3042	0.246(246)	0.1532	–	$2_3^+ \rightarrow 2_1^+$	0.0031	0.0022(2)	0.0026	0.0004
$14_1^+ \rightarrow 12_1^+$	0.4070	0.282(42)	0.2809	–	$4_2^+ \rightarrow 4_1^+$	0.1333	0.125(47)	0.1032	0.1062(14)
$16_1^+ \rightarrow 14_1^+$	0.3278	0.42(14)	0.2015	–	$6_2^+ \rightarrow 6_1^+$	0.0868	–	0.0648	–
$18_1^+ \rightarrow 16_1^+$	0.2330	0.598(105)	0.1077	–	$10_2^+ \rightarrow 10_1^+$	0.0394	–	0.0247	–
$6_2^+ \rightarrow 6_1^+$	0.1701	–	0.1329	–	$3_1^+ \rightarrow 4_1^+$	0.0799	0.096(44)	0.0618	0.0829
$3_1^+ \rightarrow 4_1^+$	0.1507	–	0.1197	–	$3_1^+ \rightarrow 2_1^+$	0.0281	0.0029(6)	0.0218	0.0034(2)
$3_1^+ \rightarrow 2_1^+$	0.0525	–	0.0419	–	$3_1^+ \rightarrow 2_2^+$	0.2000	0.3454	0.1548	0.2091(24)
$3_1^+ \rightarrow 2_2^+$	0.3766	–	0.2992	–					

is spherical, and it is distorted, when $\beta \neq 0$. The parameter γ is the amount of deviation from the focus symmetry and correlates with the nucleus shape. If $\gamma = 0$, the shape is prolate, and if $\gamma = 60$ the shape becomes oblate. In Fig. 3, the contour plots in the $\gamma - \beta$ plane resulting from $E(N, \beta, \gamma)$ are shown for $^{120-126}\text{Xe}$ isotopes. For most of the considered Xe nuclei, the mapped IBM energy surfaces are of the triaxial shape. This shape is associated with intermediate values $0 < \gamma < 60$. The triaxial deformation helps to understand the prolate-to-oblate shape transition that occurs in the considered Xe isotopes. The Xe nuclei considered here do not display any rapid structural change, but remain γ -soft. This evolution reflects the triaxial deformation, as one approaches the neutron shell closure $N = 82$.

4. Conclusions

The energy levels (positive parity), reduced probabilities of $E2$ transitions, and potential energy surfaces for $^{120-126}\text{Xe}$ nuclei have been calculated within

the framework of the interacting boson model-1. The predicted low-lying levels (energies, spins, and parities) and the reduced probabilities of $E2$ transitions are reasonably consistent with the experimental data. For the even $^{120-126}\text{X}$ isotopes, the potential energy surfaces show that all nuclei are deformed and are characterized by the dynamical symmetry $O(6)$.

We thank University of Kufa, Faculty of Education for Girls, Department of Physics and University of Kerbala, College of Science, Department of Physics for supporting this work.

1. R.B. Firestone. *Table of Isotopes CD* (Wiley, 1996).
2. F. Pan, J.P. Draayer. New algebraic solutions for $SO(6) \leftrightarrow U(5)$ transitional nuclei in the interacting boson model. *Nucl. Phys. A* **636**, 156 (1998) [DOI: 10.1016/S0375-9474(98)00207-3].
3. F. Iachello, A. Arima. Boson symmetries in vibrational nuclei. *Phys. Lett. B* **53**, 309312 (1974) [DOI: 10.1016/0370-2693(74)90389-X].
4. A. Arima, F. Iachello. Collective nuclear states as representations of a $SU(6)$ group. *Phys. Rev. Lett.* **35**, 1069 (1975) [DOI: 10.1103/PhysRevLett.35.1069].

5. R. Kumar, S. Sharma, J.B. Gupta. Character of quasi-bands in ^{150}Sm using IBM. *Arm. J. Phys.* **3(3)**, 150 (2010).
6. P. Cejnar, J. Jolie, R.F. Casten. Quantum phase transitions in the shapes of atomic nuclei. *Rev. Mod. Phys.* **82**, 2155 (2010) [DOI: 10.1103/RevModPhys.82.2155].
7. R.F. Casten, P. von Brentano. An extensive region of O(6)-like nuclei near $A = 130$. *Phys. Lett. B* **152**, 22 (1985) [DOI: 10.1016/0370-2693(85)91131-1].
8. J. Dillingg, G. Audi, D. Beck, G. Bollen, S. Henry, F. Herfurth, A. Kellerbauer, H.-J. Kluge, D. Lunney, R.B. Moore, C. Scheidenberger, S. Schwarz, G. Sikler, J. Szerypo (ISOLDE collaboration). Direct mass measurements of neutron-deficient xenon isotopes with the ISOLTRAP mass spectrometer. *Nucl. Phys. A* **701**, 520 (2002) [DOI: 10.1016/S0375-9474(01)01638-4].
9. S.A. Eid, S.M. Diab. Nuclear structure of $^{122-134}\text{Xe}$ isotopes. *Progress in Physics* **1**, 54 (2012).
10. Z.K. Pomorski, B. Nerlo-Pomorska. High spin behavior of nuclei with proton number 40–60. *Z. Phys. A* **283**, 383 (1977) [DOI: 10.1007/BF01409519].
11. B.S. Rawat, P.K. Chattopadhyay. The breaking of O(6) symmetry in ^{118}Xe and ^{120}Xe . *Pramana-J. Phys.* **53**, 911 (1999) [DOI: 10.1007/s12043-999-0125-5].
12. H. Kusakari, M. Sugawara. Study of $^{122-130}\text{Xe}$ with the extended interacting-boson approximation. *Z. Phys. A* **317**, 287 (1984) [DOI: 10.1007/BF01438360].
13. B. Sahaa, A. Dewald, O. Moller, R. Peusquens, K. Jessen, A. Fitzler, T. Klug, D. Tonev, P. von Brentano, J. Jolie, B.J.P. Gall, P. Petkov. Probing nuclear structure of ^{124}Xe . *Phys. Rev. C* **70**, 034313 (2004) [DOI: 10.1103/PhysRevC.70.034313].
14. H. Kusakari, K. Kitao, K. Sato, M. Sugawara, H. Katsuragawa. High-spin states in even-mass Xe nuclei and back-bending phenomena. *Nucl. Phys. A* **401**, 445 (1983) [DOI: 10.1016/0375-9474(83)90359-7].
15. L. Coquard, G. Rainovski, N. Pietralla, T. Ahn, L. Bettermann, M.P. Carpenter, R.V.F. Janssens, J. Leske, C.J. Lister, O. Möller, T. Möller, W. Rother, V. Werner, S. Zhu. O(6)-symmetry breaking in the γ -soft nucleus ^{126}Xe and its evolution in the light stable xenon isotopes. *Phys. Rev. C* **83**, 044318 (2011) [DOI: 10.1103/PhysRevC.83.044318].
16. M. Serris, C.T. Papadopoulos, R. Vlastou, C.A. Kalfas, S. Kossionides, N. Fotiades, S. Harissopoulos, C.W. Beausang, M.J. Joyce, E.S. Paul, M.A. Bentley, S. Araddad, J. Simpson, J.F. Sharpey-Schafer. High spin structures of ^{122}Xe . *Z. Phys. A* **358**, 37 (1997) [DOI: 10.1007/s002180050274].
17. B. Wang. Systematics of β and γ parameters of O(6)-like nuclei in the interacting boson model. *Chin. Phys. Lett.* **14**, 503 (1997).
18. R.F. Casten, D.D. Warner. The interacting boson approximation. *Rev. Mod. Phys.* **60**, 389 (1988) [DOI: 10.1103/RevModPhys.60.389].
19. F.I. Sharrad, H.Y. Abdullah, N. Al-Dahan, A.A. Mohammed-Ali, A.A. Okhunov, H.A. Kassim. SHAPE transition and collective excitations in neutron-rich $^{170-178}\text{Yb}$ nuclei. *Rom. J. Phys.* **57**, 1346 (2012).
20. F. Iachello, A. Arima. *The Interacting Boson Model* (Cambridge Univ. Press, 1987) [ISBN: 0-521-30282-X].
21. R. Bijker, A.E.L. Dieperink, O. Scholten, R. Spanhoff. Description of the Pt and Os isotopes in the interacting boson model. *Nucl. Phys. A* **344**, 207 (1980) [DOI: 10.1016/0375-9474(80)90673-9].
22. <http://www.nndc.bnl.gov/chart/getENSDFDatasets.jsp>.
23. K. Kitao, Y. Tendow, A. Hashizume. Nuclear data sheets for $A = 120$. *Nucl. Data Sheets* **96**, 241 (2002) [DOI: 10.1006/ndsh.2002.0012].
24. T. Tamura. Nuclear data sheets for $A = 122$. *Nucl. Data Sheets* **108**, 455 (2007) [DOI: 10.1016/j.nds.2007.02.001].
25. J. Katakura, Z.D. Wu. Nuclear data sheets for $A = 124$. *Nucl. Data Sheets* **109**, 1655 (2008) [DOI: 10.1016/j.nds.2008.06.001].
26. J. Katakura, K. Kitao. Nuclear data sheets for $A = 126$. *Nucl. Data Sheets* **97**, 765 (2002) [DOI: 10.1006/ndsh.2002.0020].
27. A. Arima, F. Iachello. Interacting boson model of collective nuclear states IV. The O(6) limit. *Ann. Phys. NY* **123**, 468 (1979) [DOI: 10.1016/0003-4916(79)90347-6].
28. F.I. Sharrad, H.Y. Abdullah, N. AL-Dahan, N.M. Umran, A.A. Okhunov, H. Abu Kassim. Low-lying states of ^{184}W and ^{184}Os nuclei. *Chinese Phys. C* **37**, 034101 (2013) [DOI: 10.1088/1674-1137/37/3/034101].
29. K. Abrahams, K. Allaartand, A.E.L. Dieperink. *Nuclear Structure* (Plenum Press, 1981).
30. H.R. Yazar, U. Erdem. Nature of excited states of gadolinium isotopes. *Chin. J. Phys.* **46**, 270 (2008) [DOI: 10.6122/CJP].
31. W.D. Hamilton. *The Electromagnetic Interaction in Nuclear Spectroscopy* (American Elsevier Publishing Company, 1975) [ISBN: 444-10519].
32. L. Coquard. *Ph.D. thesis* (Technical Univ. Darmstadt, 2010).

Received 07.10.16

*X.X. Худер, А.К. Hasan, Ф.І. Шаррад*РОЗРАХУНОК РІВНІВ ЕНЕРГІЙ, ІМОВІРНОСТЕЙ ПЕРЕХОДУ, ПОВЕРХОНЬ ПОТЕНЦІАЛЬНОЇ ЕНЕРГІЇ ДЛЯ ПАРНО-ПАРНИХ $^{120-126}\text{Xe}$ ІЗОТОПІВ

Р е з ю м е

У моделі взаємодіючих бозонів розраховано рівні енергії, ймовірності переходів $B(E2)$ і поверхні потенціальної енергії деяких парних $^{120-126}\text{Xe}$ ізотопів у хорошій відповідності до експериментальних даних. Поверхня потенціальної енергії як одна з характеристик ядра визначає кінцеву форму ядер. Контурний графік поверхонь потенціальної енергії показує, що $^{120-126}\text{Xe}$ ядра деформовані і нестабільні до γ -розпадів.